Scientific Research Publishing

Materials Sciences and Applications, 2019, 10, 205-215
http://www.scirp.org/journal/msa
ISSN Online: 2153-1188
ISSN Print: 2153-117X

Strain Rate Effects on Tensile Properties of HDPE-PP Composite Prepared by Extrusion and Injection Moulding Method

Harekrushna Sutar[1*], Himanshu Sekhar Maharana[2], Chiranjit Dutta[3], Rabiranjan Murmu[1], Sangram Patra[1]

[1]Chemical Engineering Department, Indira Gandhi Institute of Technology, Sarang, India
[2]Materials Science and Engineering Department, Indian Institute of Technology, Kanpur, India
[3]Chemical Engineering Department, National Institute of Technology, Trichy, India
Email: *h.k.sutar@gmail.com

How to cite this paper: Sutar, H., Maharana, H.S., Dutta, C., Murmu, R. and Patra, S. (2019) Strain Rate Effects on Tensile Properties of HDPE-PP Composite Prepared by Extrusion and Injection Moulding Method. *Materials Sciences and Applications*, **10**, 205-215.
https://doi.org/10.4236/msa.2019.103017

Received: February 11, 2019
Accepted: March 9, 2019
Published: March 12, 2019

Abstract

The present paper investigates the effect of strain rate on different tensile properties of high density polyethylene (HDPE) and polypropylene (PP) composite. Tensile specimens of virgin HDPE-PP composites are prepared via twin screw extruder and injection moulding methods as per ASTM D638-02a (Type-I); with gage length 50 mm, width 13 mm and thickness 3 mm. Composites are fabricated with PP as reinforcing agent at a loading rate of 10%, 20%, 30%, 40% and 50% by weight. Experiments are carried out at room temperature of 23˚C and absolute humidity of 54% at a cross head speed of 30, 40, 50, 60 and 70 mm/min. Stress and strain values at yield and break points are reported. Atomic force microscopy (AFM) is used to study the distribution of polymer molecules in the mixture and surface roughness. As in last, experiments are designed by Taguchi optimization method to find out the dominating factors on tensile strength.

Keywords

HDPE-PP Blend, Strain Rate, Tensile Strength, AFM, DOE

1. Introduction

History reveals, the composites are mainly used for savings in secondary structures. The fibre-reinforced polymer (FRP) materials find increasing applications as load bearing structures. But in the other hand, development of polymer materials for high technology engineering applications is in demand [1] [2] [3]. It is always a matter of concern, to evaluate the mechanical properties of polymer

composites at high rates of strain. Premature failure at high loading rates alarms to design structures with high strength. The progress in research to find the mechanical strength of thermoplastic polymer blends are still lacks. With respect to above argument, a polymer blend of HDPE-PP has been developed to understand the strain rate effects on particularly to tensile properties.

A detailed review of the strain rate dependence of mechanical properties of polymer composites has been outlined by Jacob *et al.* [4]. The study of different properties of polymer blends is a new approach [5]. These polymeric materials must perform at the imposed conditions. Blend of HDPE-PP has been prepared [6] [7] and its mechanical, thermal, crystallization and electrical properties has been studied. An experimental approach using universal testing machine (UTM) was employed to study the effect of low strain rate loading on HDPE/saw dust composites [8]. In fibre reinforced polymer composites, the increment of filler may increase its tensile strength [9]. In general, the filler is incapable to endure the stress transmission efficiently and resulting low compression strength [10] [11]. In a similar manner, Bia *et al.* [12] studied the tensile properties of rigid glass bead/HDPE composites at a strain rate of 3×10^{-5} - 8×10^{-3} s^{-1} and observed tensile modulus and strength increases with loading rate. Over the last two decades, the global production of synthetic polymers increasing. Polymers have low weight, durability and cheap relative to other materials [13] [14] [15]. So in the present work an attempt has been made to find out an alternative use of HDPE-PP polyblend by accessing the tensile properties at different strain rates. Additionally the design of experiments (DOE) is carried out to discover the influencing factor on tensile strength at break point.

2. Materials and Method

2.1. Polymeric Raw Materials

Virgin PP of M110 Grade (homopolymer) produced by the sphericol technology and virgin HDPE of M5818 Grade (injection moulded type) produced by Mitsui Slurry CX technology are purchased from Haldia petrochemical limited, Haldia, West Bengal, India. Typical physical properties of the polymers are reported in Table 1.

2.2. Tensile Specimen Preperation

Polymers are collected in the form of pellets. The pellets are dried in a hot air oven at 60˚C for 8 hrs to remove moisture content followed by mixing of 10, 20, 30, 40 and 50 wt. % of PP to HDPE. Then they are mixed using a twin screw extruder (ZV20, Specific Engineering and Auto Mates, Vadodara, India) at feeder

Table 1. Physical properties of polymers.

Polymer type	Melt flow index (g/10 min)	Density (g/cc)
HDPE	19 (2.16 kg, 190˚C)	0.956
PP	11 (2.16 kg, 230˚C)	0.90

speed of 51 rpm and main rotor at 54 rpm to form a homogeneous polymer blend and are collected in the form of pellets. The screws are of 21 mm diameter and co-rotating type, containing three thermal barrels at 190˚C, 200˚C and 210˚C respectively. The melt and die temperatures are 224˚C and 200˚C.

The obtained pellets are moulded immediately to tensile test samples using an automatic injection moulding machine (Endura-90, Electonica plastic machines limited, Kolkata, India) with screw diameter of 35 mm at 177 rpm. The temperature of the nozzle is 200˚C and that of the three barrels are 190˚C, 200˚C and 210˚C respectively. Tensile specimens are prepared according to ASTM D638-02a type-I (gage length 50 mm, with 13 mm and thickness 3 mm) standard.

2.3. Prediction of Tensile Properties

Tensile characteristics of HDPE/PP polyblends are determined using an universal testing machine (UTM-3382, Instron, UK). Tests are conducted at cross head speed of 30, 40, 50, 60 and 70 mm/min for each composite type at atmospheric temperature of 23˚C and absolute humidity of 54%. Stress and strain at yield and break points are estimated in the experiment and reported in result and discussion section. Each data corresponds to the mean value for three independent observations.

2.4. Atomic Force Microscopy (AFM)

We have used AFM (Park XE 100, South Korea) to observe the topography of prepared tensile specimens. In order to see the surface behaviour of the specimens, i.e. the distribution of polymer molecules in the blend and root mean square (rms) roughness (R_q) in nanometre scale; an AFM at non contact mode and room temperature is implemented. Images were scanned by using a cantilever of tip radius 10 nm (NCHR mode), a nominal spring constant of 0.05 N/m and a scanning rate of 0.9 Hz. The scans were made on 1000 nm × 1000 nm scale (except for 60HDPE/40PP, held at 750 nm × 750 nm) and repeated five different times on five different area of the polymer surface (tensile specimen) at a resolution of 256 × 256 pixels (except for 60HDPE/40PP, held at 192 × 192 pixels) , set point of 10 nm, amplitude of 20.85 nm. The rms roughness is determined [16] by following equation,

$$\text{rms} = \frac{\sqrt{\left(Z_i - Z_{av}\right)^2}}{N} \tag{1}$$

where, Z_i is the height at a particular point on an image (nm), Z_{av} is the mean height of all pixels in the image (nm) and N is the total number of pixels in the image. The maximum range is the height difference between the lowest and highest pixels in the image.

2.5. Taguchi Optimization

DOE is one of the powerful statistical techniques to study the influence of the

controlling factor on output. All designed experiments require a certain number of combinations of factors and levels to be tested in order to observe the results of those test combination. In our project, Taguchi optimization method is employed to find out the optimum operating parameters influencing the tensile properties using MINITAB-16 software. Tensile strength at break point is considered as response. The operating conditions implemented are given in Table 2.

Full-Factorial design is conducted in accordance with 5 level L_{25} (5^6) orthogonal array. The S/N ratios for maximum tensile strength at break (in MPa) under "larger is the better characteristic" are calculated as the logarithmic transformation of the loss function as shown below.

Larger is the better characteristic:

$$\frac{S}{N} = -10\log\frac{1}{n}\left(\sum\frac{1}{Y^2}\right) \tag{2}$$

where "n" is the repeated number trial conditions and "Y" is the data pertaining to tensile strength at break point.

3. Results and Discussion

2D and 3D topography of the prepared tensile specimens are seen, and reported in Figure 1. The polymers are uniformly distributed inside the composite as visible in the AFM images. The white and brown spots (both dark and dull) are confirming to the PP and HDPE phases respectively. Few aggregative PP phases are observed in the 50HDPE/50PP composite. A wide distribution of PP molecules within the blend is noticeable in 90% HDPE blend (Figure 1(i) and Figure 1(j)). As both the polymers are not compatible to each other, the molecular distribution of PP declines with its content. HDPE holds low melting point and high melt flow index, resulting a smoother surface formation during injection moulding. Results corresponding to the rms roughness (R_q) are revealed in Figure 2.

Attributing to the above discussion, the roughness of the prepared tensile specimen confirms to be minimum for 90HDPE/10PP polymer composite. The maximum rms roughness (R_q = 3.478 nm) is resulting for 50HDPE/50PP polyblend specimen and falls with increase in HDPE load. Data pertaining to the tensile properties conducted using the UTM, are reported in Table 3 and Table 4. Table 3 shows the outcomes for the tensile stress at yield and break points in MPa. The resulted strain in % at both yield and break points are disclosed in Table 4.

The optimisation result shows that tensile strength is maximum for 50HDPE/50PP polyblend. The tensile strength decreases with increase in HDPE

Table 2. Levels of the variables used in the experiment.

Control Factors	Level					
	1	2	3	4	5	Units
Composition (code: C)	50	60	70	80	90	Weight % (HDPE)
Speed (code: S)	30	40	50	60	70	mm/min

Table 3. Experimental values of Stress at yield and break point.

Composite	Speed, mm/min									
	30	40	50	60	70	30	40	50	60	70
	Stress, MPa									
	At Yield					At break				
50HDPE/50PP	27.96	25.40	27.42	26.42	27.49	25.73	23.22	26.69	25.57	26.12
60HDPE/40PP	23.74	24.53	24.85	25.60	25.78	14.39	13.07	6.26	6.85	6.44
70HDPE/30PP	25.73	26.11	26.78	27.47	27.15	23.57	24.29	24.15	25.50	25.17
80HDPE/20PP	24.20	24.60	25.00	25.15	25.65	20.63	20.40	22.10	21.79	23.99
90HDPE/10PP	27.95	28.54	29.13	29.45	29.48	2.94	3.03	5.66	5.40	7.62

Table 4. Experimental values of strain at yield and break point.

Composite	Speed, mm/min									
	30	40	50	60	70	30	40	50	60	70
	Strain, %									
	At Yield					At break				
50HDPE/50PP	7.55	7.62	7.05	7.62	7.15	11.46	12.08	8.82	9.81	9.78
60HDPE/40PP	8.25	8.24	8.22	8.07	7.74	438.18	438.64	295.80	141.05	92.132
70HDPE/30PP	7.87	7.11	7.50	7.15	7.04	12.98	10.90	12.59	11.13	11.53
80HDPE/20PP	8.54	8.20	7.70	7.59	7.54	15.19	15.26	12.82	12.15	11.07
90HDPE/10PP	7.28	7.16	6.94	6.91	7.00	104.35	84.15	62.59	68.24	55.07

content in the composite. Tensile strength is minimum at the cross head speed of 40 mm/min and maximum at 70 mm/min. The Figure 3 reveals, the strength is almost same at cross head speed of 40, 50 and 60 mm/min. But the improvement of the tensile strength at the rate of 70 mm/min is quite significant. Analysis of result from Figure 3 concludes that a factor combination of C1 and S5 shows the maximum strength at break point. The results are in accordance to the fact that, high strain rates favour the elastic behaviour of materials. Elasticity is associated with load bearing performance as embodied in properties such as strength. But low strain rates favour the viscous behaviour. In our experiment; as cross head speed increases to 70 mm/min; the temperature of the specimen might declines to minimum and making it stronger and stiffer.

The tensile strength behaviour at break point is designed and reported in Table 5. S/N ratio in Taguchi's technique indicates the ranking of parameters based on their influences. The mean of the S/N ratios is found to be 22.960 dB. Response table for S/N ratios is shown in Table 6. Larger the better characteristic is taken for this analysis. The difference between the highest and lowest value estimates the magnitude of delta (Δ). Ranking was allotted in descending order with respect to the delta values. It is concluded that composition dominates in a higher extent to tensile strength; than that of cross head speed. Figure 3 and Figure 4 depicts the main effect plot for S/N ratio and mean S/N ratio respectively.

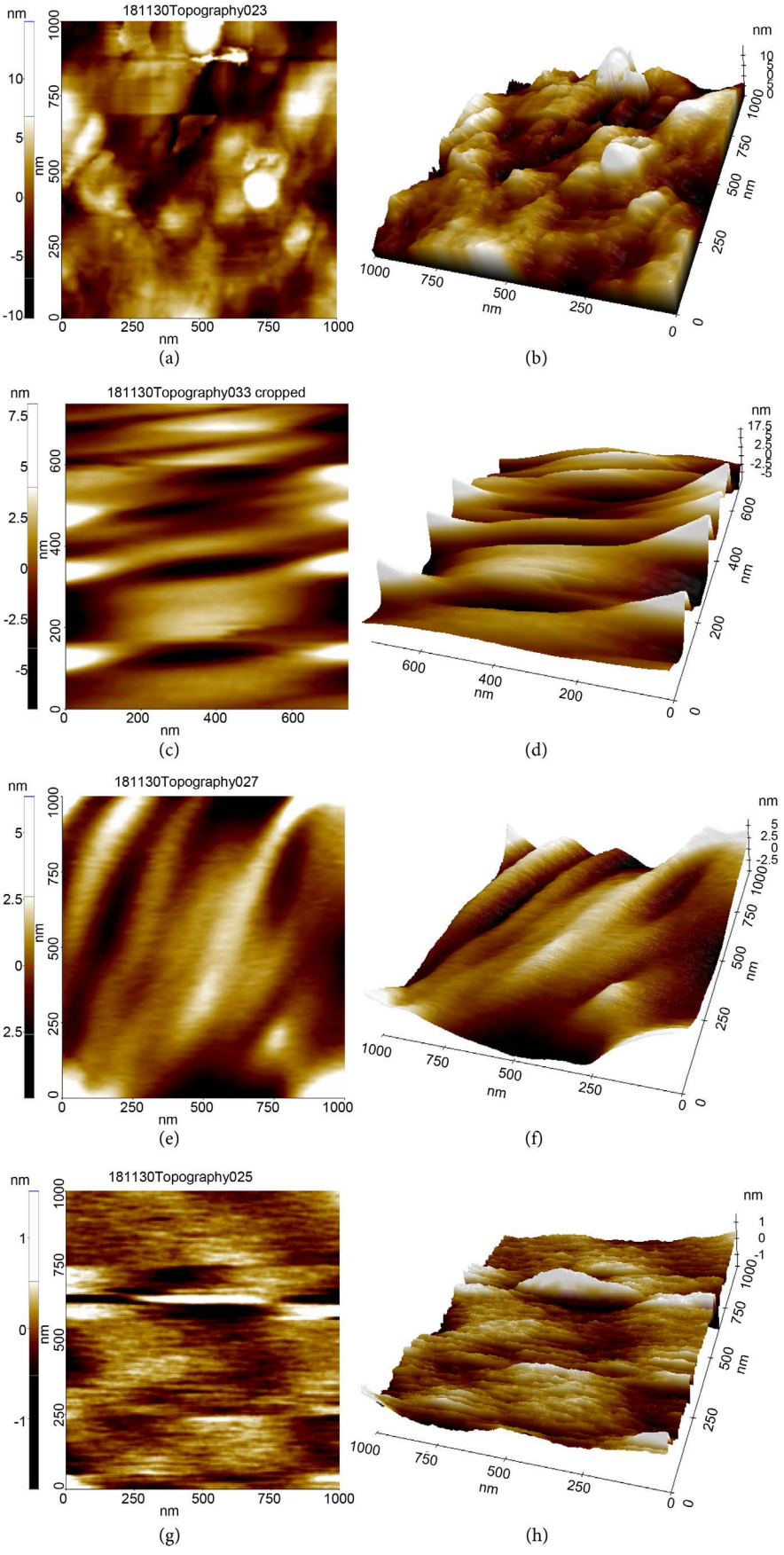
181130Topography023
nm
(a)
(b)
181130Topography033 cropped
(c)
(d)
181130Topography027
(e)
(f)
181130Topography025
(g)
(h)

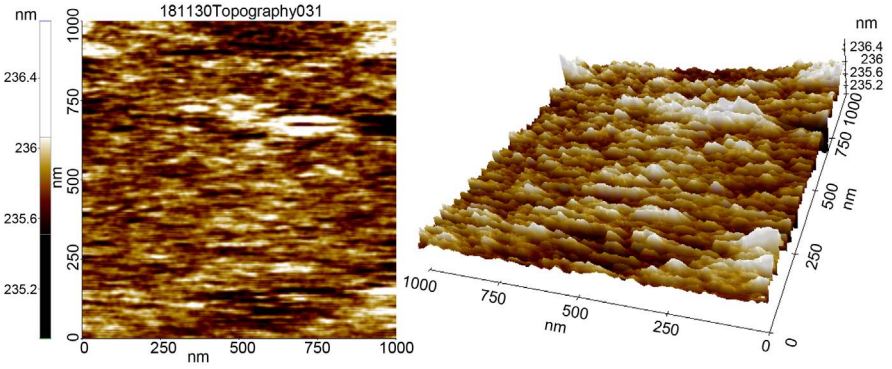

Figure 1. 2D and 3D Tapping mode AFM images of (a) (b) 50HDPE/50PP; (c) (d) 60HDPE/40PP; (e) (f) 70HDPE/30PP; (g) (h) 80HDPE/20PP; (i) (j) 90HDPE/10PP polyblends.

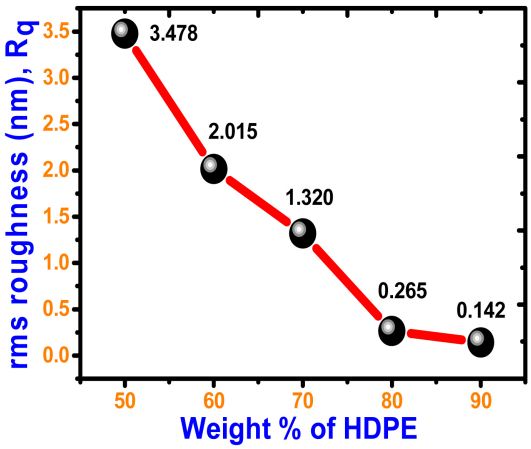

Figure 2. Root mean square roughness (R_q) of the prepared tensile specimens.

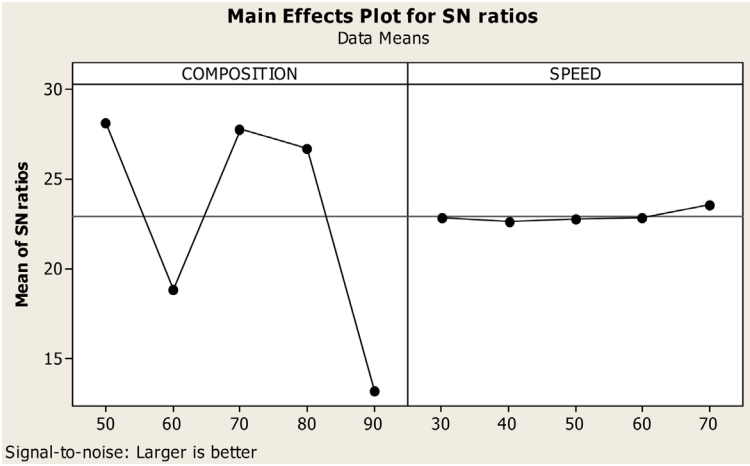

Figure 3. Main effect plot for S/N ratio.

The analysis of variance (ANOVA) is used to analyze the influence of tensile strength parameters like composition and speed. The ANOVA establishes the

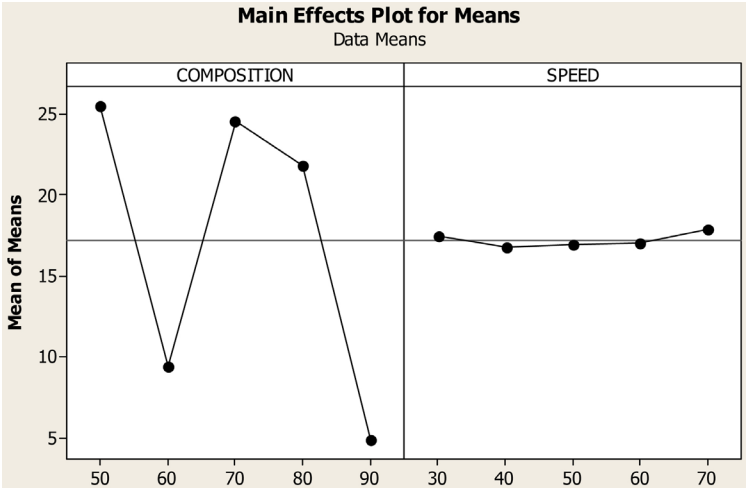

Figure 4. Main effect plot for means.

relative significances of factors in terms of their percentage contribution to the response. This analysis was carried out for a level of significance of 5% (the level of confidence 95%). "P" value, less than 0.05 for a particular parameter, indicates that it has the major effect on the responses. From **Table 7** it is observed that "P" value for the factor composition is much lesser than 0.05; so the major controlling parameter for tensile strength is composition followed by speed.

A correlation between tensile strength at break point "TS_b" (non-variable factor), composition and speed (variable factors) is derived by multiple linear regressions from equation No-3. From equation No-4, it is observed that the factor "composition" has a major impact on tensile strength followed by speed.

$$TS_b = K_0 + K_1 A + K_2 B + K_3 C \tag{3}$$

where, $K_i \left(i = 0,1,2,3,\cdots\right)$ is a model constant. The regression equation is given by

$$TS_b = 36.8 - 0.287 \text{ COMPOSITION} + 0.010 \text{ SPEED} \tag{4}$$

Finally a confirmation test was conducted to evaluate the design parameters influencing the response. The purpose of confirmation experiment is to validate the conclusions drawn during the analysis phase. For this, control parameters with optimal levels of 60HDPE/40PP for composition and 40 mm/min for speed are considered. **Table 8** shows the confirmation test result. The experimental result shows an improvement in tensile strength at break point to be 1.6%.

4. Conclusion

Our work remarks some salient features of the prepared polyblends. It is concluded that, the tensile strength decreases with increase in HDPE content. In summary, cross head speed is an important variable to decide the tensile behaviour. Tensile strengths at break point are quite identical at 40, 50 and 60 mm/min and the value is maximum at 70 mm/min. The results are quite obvious due to the earlier stated reasons. Surface roughness of the tensile specimens is

Table 5. Experimental design using L_{25} orthogonal array.

L_{25} (5^6)	Composition, Wt % HDPE	Speed, Mm/min	Tensile Strength At break, MPa	S/N Ratio, dB
1	50	30	25.73	28.21183
2	50	40	23.22	27.31986
3	50	50	26.69	28.52892
4	50	60	25.57	28.15631
5	50	70	26.12	28.33946
6	60	30	14.39	23.16423
7	60	40	13.07	22.32551
8	60	50	6.26	15.93981
9	60	60	6.85	16.72015
10	60	70	6.44	16.18581
11	70	30	23.57	27.44977
12	70	40	24.29	27.70927
13	70	50	24.15	27.65942
14	70	60	25.50	28.13217
15	70	70	25.17	28.01973
16	80	30	20.63	26.29251
17	80	40	20.40	26.19431
18	80	50	22.10	26.88824
19	80	60	21.79	26.76634
20	80	70	23.99	27.6006
21	90	30	2.94	9.378756
22	90	40	3.03	9.654614
23	90	50	5.66	15.0686
24	90	60	5.40	14.6527
25	90	70	7.62	17.64594

Table 6. Response table for tensile strength at break.

Level	COMPOSITION: C	SPEED: S
1	28.11	22.9
2	18.87	22.64
3	27.79	22.82
4	26.75	22.89
5	13.28	23.56
Delta (Δ)	14.83	0.92
Rank	1	2

significantly affected by the presence of PP; as dispersed phase in the composite. The polyblend having 50 weight % of PP and HDPE holds the highest rms roughness during moulding. Due to low material cost and traditional fabrication

Table 7. ANOVA table for tensile strength at break point.

Source	DF	Seq SS	Adj SS	Adj MS	F	P
COMPOSITION	4	873.54	873.54	218.38	33.83	0
SPEED	4	2.45	2.45	0.61	0.09	0.983
Error	16	103.29	103.29	6.46		
Total	24	979.28				

DF: Degree of Freedom; seq SS: The Sequential Sum of Squares; Adj SS: Adjusted Sum of Squares; Adj MS: Adjusted Mean Squares.

Table 8. Results of the confirmation experiment.

	Optimal control parameters	
	Prediction	Experimental
Level	C_2S_2	C_2S_2
S/N ratio, dB	22.85	23.22

methods, the polymer composites may find suitable applications areas.

Conflicts of Interest

The authors declare no conflicts of interest regarding the publication of this paper.

References

[1] Favaro, S., Pereira, A., Fernandes, J., Baron, O., da Silva, C., Moisés, M. and Radovanovic, E. (2017) Outstanding Impact Resistance of Post-Consumer HDPE/Multilayer Packaging Composites. *Materials Sciences and Applications*, **8**, 15-25. https://doi.org/10.4236/msa.2017.81002

[2] Erbetta, C.D.C., Azevedo, R.C.S., Andrade, K.S., eSilva, M.E.S.R. and Roberto, F.S. (2017) Characterization and Lifetime Estimation of High Density Polyethylene Containing a Prodegradant Agent. *Materials Sciences and Applications*, **8**, 979-991. https://doi.org/10.4236/msa.2017.813072

[3] Mendes, L and Cestari, S. (2011) Printability of HDPE/Natural Fiber Composites with High Content of Cellulosic Industrial Waste. *Materials Sciences and Applications*, **2**, 1331-1339. https://doi.org/10.4236/msa.2011.29181

[4] Jacob, G.C., Starbuck, J.M., Feller, J.F., Simunovic, S. and Boeman, R.G. (2004) Strain Rate Fffects on the Mechanical Properties of Polymer Composite Materials. *Journal of Applied Polymer Science*, **94**, 296-301. https://doi.org/10.1002/app.20901

[5] Salih, S., Hamood, A. and Alsalam, A. (2013) Comparison of the Characteristics of LDPE: PP and HDPE: PP Polymer Blends. *Modern Applied Science*, **7**, 33-42. https://doi.org/10.5539/mas.v7n3p33

[6] Sahoo, P.C., Murmu, R., Patra, S.C., Dutta, C. and Sutar, H. (2018) Electrical Behaviour and Spherulites Morphology of HDPE/PP Polyblends with HDPE as Base Material. *Materials Sciences and Applications*, **9**, 837-843. https://doi.org/10.4236/msa.2018.910060

[7] Sutar, H., Sahoo, P.C., Sahu, P.S., Sahoo, S., Murmu, R., Swain, S. and Mishra, S.C. (2018) Mechanical, Thermal and Crystallization Properties of Polypropylene (PP)

Reinforced Composites with High Density Polyethylene (HDPE) as Matrix. *Materials Sciences and Applications*, **9**, 502-515. https://doi.org/10.4236/msa.2018.95035

[8] Omar, M.F., Jaya, H., Akil, H.M., Ahmad, Z.A. and Noriman, N.Z. (2015) Mechanical Properties of High Density Polyethylene (HDPE)/Sawdust Composites under Wide Range of Strain Rate. *Applied Mechanics and Materials*, **754-755**, 83-88. https://doi.org/10.4028/www.scientific.net/AMM.754-755.83

[9] Abdel-Hakim, A.A., Abdel-Salam Sabbah, I., Metwally, M.S., El Begawy, S. and Elshafie E.S. (2012) Mechanical Properties and Morphology Studies of Nanocomposites Based on RSF/Nanoclay Modified /HDPE Nanocomposites. *Life Science Journal*, **9**, 134-142.

[10] Rahman, M.R., Islam, M.N., Huque, M.M., Hamdan, S. and Ahmed, A.S. (2010) Effect of Chemical Treatment on Rice Husk (RH) Reinforced Polyethylene (PE) Composites. *BioResources*, **5**, 854-869.

[11] Yang, H.S., Kim, H.J., Son, J., Park, H.J., Lee, B.J. and Hwang, T.S. (2004) Rice-Husk Flour Filled Polypropylene Composites; Mechanical and Morphological Study. *Composite Structures*, **63**, 305-312. https://doi.org/10.1016/S0263-8223(03)00179-X

[12] Bai, S.L., Cao, K., Chen, J.K. and Liu, Z.D. (2000) Tensile Properties of Rigid Glass Bead/HDPE Composites. *Polymers and Polymer Composites*, **8**, 413-418.

[13] Reis, J.M.L., Pacheco, L.J. and da Costa Mattos, H.S. (2013) Influence of the Temperature and Strain Rate on the Tensile Behavior of Post-Consumer Recycled High-Density Polyethylene. *Polymer Testing*, **32**, 1576-1581. https://doi.org/10.1016/j.polymertesting.2013.10.008

[14] Siviour, C.R. and Jordan, J.L. (2016) High Strain Rate Mechanics of Polymers: A Review. *Journal of Dynamics Behaviour of Materials*, **2**, 15-32. https://doi.org/10.1007/s40870-016-0052-8

[15] Dhoble, A., Kulshreshtha, B., Ramaswami, S. and Zumbrunnen, D.A. (2005) Mechanical Properties of PP-LDPE Blends with Novel Morphologies Produced with a Continuous Chaotic Advection Blender. *Polymer*, **46**, 2244-2256. https://doi.org/10.1016/j.polymer.2005.01.057

[16] Al Maadeed, M.A., Labidi, S., Krupa, I. and Ouederni, M. (2015) Effect of Waste Wax and Chain Structure on the Mechanical and Physical Properties of Polyethylene. *Arabian Journal of Chemistry*, **8**, 388-399. https://doi.org/10.1016/j.arabjc.2014.01.006